ACS APPLIED MATERIALS & INTERFACES

Research Article

www.acsami.org

Additional Molecular Biological Amplification Strategy for Enhanced Sensitivity of Monitoring Low-Abundance Protein with Dual Nanotags

Bing Zhang, Bingqian Liu, Jun Zhou, Juan Tang, and Dianping Tang*

Key Laboratory of Analysis and Detection for Food Safety, Fujian Province & Ministry of Education of China, Department of Chemistry, Fuzhou University, Fuzhou 350108, China

ABSTRACT: A new signal-on immunoassay protocol for sensitive electronic detection of alpha-fetoprotein (AFP) was developed by coupling with metal sulfide nanolabels and a silver nanocluster (AgNC)-based rolling circle amplification (RCA) strategy. Initially, a sandwiched immunocomplex was formed on a primary antibody-coated microplate using a PbS nanoparticle-labeled polyclonal anti-AFP antibody (PbS-pAb_2) as the detection antibody, and then the carried PbS-pAb_2 was dissolved by acid to release a large number of lead ions, which could induce the cleavage of lead-specific DNAzyme immobilized on the electrode. The residual single-stranded DNA on the electrode could be used as the primer to produce numerous repeated oligonucleotide sequences via the RCA reaction for the hybridization with many AgNC-labeled detection probes, resulting in the amplification of the electronic signal due to the unique properties of silver nanoclusters. Under optimal conditions, the developed immunoassay exhibited high sensitivity for the detection of AFP with a dynamic range of 0.001−200 ng mL^{-1} and a detection limit (LOD) of 0.8 pg mL^{-1}. Intra-assay and interassay coefficients of variation were below 8.0% and 10%, respectively. Importantly, the methodology was evaluated by analyzing 12 clinical serum specimens, and no significant differences were encountered in comparison with the conventional enzyme-linked immunosorbent assay (ELISA) method.

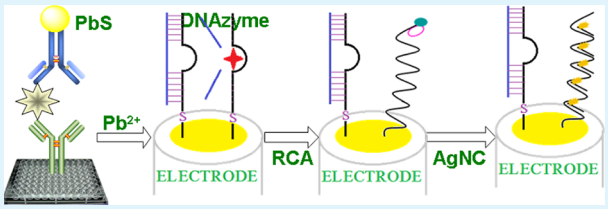

KEYWORDS: *electrochemical immunoassay, metal sulfide nanoparticles, silver nanoclusters, low-abundance protein, rolling circle amplification*

1. INTRODUCTION

Sensitive and specific determination of low-abundance protein in biological fluids is of immense significance in the early diagnosis of disease.[1,2] To date, the complexity of the plasma proteome exceeds the analytical capacity of conventional approaches to isolate lower abundance proteins that may prove to be informative biomarkers. Immunoassay based on the antigen−antibody reaction is one of the most important analytical techniques in the quantitative detection of low-abundance protein due to the highly specific molecular recognition of immunoreaction.[3,4] Although the interaction between the antibody and the corresponding antigen causes the production of the signal to some extent, the signal change is usually very little.[5] To meet the requirement of clinical diagnostics, the detectable signal amplification is very important.

Recently, various signal amplification methods and strategies have been reported for this purpose, such as enzyme labeling, nanolabeling, and molecular biological amplification.[6−9] Undoubtedly, enzyme labeling is one of most widely used protocols because a single enzymatic molecule, for example, horseradish peroxidase, may cause the conversion of 10^7 molecules of substrate per minute.[10] In contrast, one major merit of using nanolabeling is that one can control and tailor their properties in a very predictable manner to meet the needs of specific applications.[11,12] Significantly, a molecular biological method was also employed as the signal amplification protocol for the determination of biomolecules, e.g., by using DNA-based thermal cycling or isothermal cycling techniques.[13,14]

DNAzyme is a specific single-stranded DNA sequence that can catalyze chemical and biological reactions.[15,16] One interesting example is "8−17" DNAzyme whose catalytic activities can be specifically regulated by lead ion,[17] The specificity of DNAzyme can be utilized for selective determination of lead ions.[18−20] Inspiringly, the metal ions can be usually obtained based on the corresponding metal sulfide quantum dots by acid, which provide an advantageous convenience for the development of nanolabeling (because the quantum dots are comprised of numerous metal ions). Most recently, we reported a new electrochemical immunoassay protocol based on cleavage of metal ion-induced DNAzyme released from nanolabels.[21] The signal was amplified by the labeled ferrocene redox tag on the DNAzyme due to the conformational change of DNAzyme after cleavage. Although one PbS quantum dot could cause the cleavage of many DNAzymes, the amount of the labeled ferrocene tags were limited because one DNAzyme was conjugated with only one ferrocene molecule. In this regard, our motivation in this work

Received: March 20, 2013
Accepted: April 17, 2013
Published: April 17, 2013

was to adequately utilize the cleaved DNA strand for further signal amplification by using a molecular biological strategy.

Rolling circle amplification (RCA) is a unique enzymatic process that can be used to generate extremely long single-stranded DNA (ssDNA) with repeating sequences.[22,23] This process is carried out with a short DNA primer and a circular DNA template under isothermal conditions by a special DNA polymerase with strong strand-displacement ability.[24,25] On the basis of its simplicity, robustness, specificity, and high sensitivity, RCA gained considerable attention as a new molecular biological amplification tool for the detection of biomolecules.[26−28] Herein, we report the proof-of-concept of a novel and powerful electrochemical immunoassay for the detection of alpha-fetoprotein (AFP, as a model) by coupling the cleavage of lead ion-induced DNAzymes released from a PbS nanoparticle-labeled detection antibody with a silver nanocluster-based rolling cycling amplification strategy. The assay is implemented as follows: (i) the formation of an immunocomplex with PbS nanolabels in the microplate, (ii) the release of lead ions from the nanolabels, (iii) cleavage of Pb^{2+}-specific DNAzymes on the electrode, (iv) RCA reaction with silver nanoclusters, and (v) electrochemical measurement. The detectable signal is expected to be amplified by using PbS nanolabels and silver nanoclusters. The aim of this study is to realize the continuous amplification of detectable signals for the detection of low-abundance protein.

2. EXPERIMENTAL SECTION

Monoclonal mouse anti-human AFP antibody (mAb_1) and polyclonal rabbit anti-human AFP antibody (pAb_2) were purchased from Abgent (Amyjet Sci., Inc., China). AFP standards with various concentrations were obtained from Biocell Biotechnol. Co., Ltd. (Zhengzhou, China). *N*-(3-dimethylamminopropyl)-*N*′-ethyl-carbodiimide hydrochloride (EDC), diethylene glycol (DEG, 99%), *N*-hydroxysulfosuccinimid sodiumsalt (NHS), polyacylic acid (PAA), and thiourea (TU, 99%) were purchased from Alfa Aesar. Deoxyribonucleoside 5′-triphosphates mixture (dNTP) and phi29 DNA polymerase were purchased from Takara Biotechnol. Co., Ltd. (Dalian, China). All other chemicals were of extra pure analytical grade and used without further purification. All solutions were prepared with deionized water obtained from a Milli-Q water purifying system (≥18 MΩ, Milli-Q, Millipore). The washing buffer solution was a 0.01 M phosphate-buffered saline (PBS, pH 7.4) solution containing 0.05% Tween 20. The blocking buffer was 0.01 M PBS (pH 7.4) containing 2.5 wt % BSA. Tris-acetic acid stock buffer and PBS buffer were the products of Sigma-Aldrich. Clinical serum samples were made available by Fujian Provincial Hospital, China.

All oligonucleotides used in the experiments were obtained from Sangon Biotech. Co., Ltd. (Shanghai, China). The sequences of oligonucleotides are listed as follows:

Catalytic strand: 5′- HS-TTT CAT CTC TTC TCC GAG **CCG GTC GAA ATA GTG AGT**-3′
Substrate strand: 5′-ACT CAC TAT **rA** GGA AGA GAT G-3′
Circular template: 5′-p-*TTC GAC CGG* AAC TGT CTT AGC AAA AAC TGT CTT AGC AAA *CTC ACT AT*-3′
Detection probe: 5′-*CAC TAT TTC GAC* **CCC CAA CTC CCC**-3′

The design of DNAzyme molecular beacons was adapted from the literature.[19,29] In the molecular beacons, lead ion-specific catalytic strands (36 bases) and substrate strands with ribo-adenosine (rA) (19 bases) were designated as Pb-Enz and Pb-Sub, respectively. The boldface portion at the catalytic strand is the primer sequence for the RCA reaction. The italicized portion at the circular template (p = 5′ phosphate) matches the italicized sequence of the catalytic strand. The italicized portion at the detection probe is the same as those in italic on the circular template. The boldface portion at the detection probe is for the preparation of silver nanoclusters.

Before preparation of PbS-pAb_2 conjugates, the carboxylated PbS nanoparticles were initially synthesized according to our recent report.[21] Briefly, solution A containing thiourea (8.0 mmol) and diethylene glycol (20 mL, 99.9 wt %) was initially heated to 100 °C for 60 min under N_2 and then cooled to room temperature (RT). Solution B was prepared by mixing 0.4 mmol Pb(II) acetate, 6.0 mmol PAA, and 6.0 mL DEG, which was heated to 215 °C under N_2. Following that, 8.0 mL of solution A was injected rapidly into the hot solution B. Upon addition of solution B, the mixture turned black quickly. Afterward, the mixture was heated to 210 °C for 15 min. Subsequently, the suspension was cooled to RT and centrifuged 10 min at 11,000*g*. Finally, the water-soluble carboxylated PbS nanoparticles were obtained, and 2.0 mL of distilled water was dispersed for further use.

Next, the as-synthesized PbS nanoparticles were utilized for labeling of the mAb_2 antibody by using the classical carbodiimide coupling method. Initially, 2.2 mg of NHS and 3.0 mg of EDC were dissolved into 500 μL of PbS colloids, followed by continuous stirring for 45 min at RT. Afterward, 100 μL of pAb_2 (0.5 mg mL^{-1}) was added into the mixture, and the mixture was gently stirred for 12 h to make pAb_2 conjugate onto the PbS nanoparticles. The excess chemicals and antibodies were removed by centrifugation. Finally, the as-prepared PbS-pAb_2 nanolabels were dispersed into 1.0 mL PBS (0.1 M, pH 7.4) for detection of AFP in the following experiments.

Silver nanocluster (AuNC) was in situ synthesized by using a DNA detection probe based on the C−Ag^+−C principle according to the literature.[30] Briefly, 50 μL of detection probe (100 μM, 5′-CAC TAT TTC GAC CCC CAA CTC CCC-3′) and 0.8 μL of $AgNO_3$ solution (25 mM) were initially added into 50 μL of citrate buffer (20 mM, pH 7.0) with a Ag^+/oligonucleotide relative concentration ratio of 4:1, and then the mixture was gently shaken for 30 min at RT. During this process, the C−Ag^+−C was formed at the 3′ end. Following that, 0.8 μL of fresh $NaBH_4$ solution (25 mM) was added to the mixture in an ice bath, and the resulting solution was vigorously shaken for 1 min. Finally, the oligonucleotide-encapsulated silver nanoclusters (designated as Ag-DNA) were obtained by keeping the solution overnight in the dark at 4 °C.

A cleaned gold electrode (3 mm in diameter) was initially immersed into a 0.2 M Tris-HCl buffer (pH 7.4) containing 2.0 OD Pb-Enz and 8.0 mM tris-(2-carboxyethyl) phosphine hydrochloride for 16 h. After rising with washing buffer, the modified gold electrode was incubated with 1.0 mM 6-mercaptohexanol in a 10 mM Tris-acetate buffer, pH 7.4, for 60 min. Following that, the Pb-Enz-modified electrode was dipped again into 2.0 OD Pb-Sub in order to make the Pb-Enz hybridize with the Pb-Sub in an oven at 65 °C for 10 min. Afterward, the hybridization was further carried out at RT for 12 h. Finally, the obtained DNAzyme sensor was stored at 4 °C when not in use.

Scheme 1. Schematic Illustration of Three Different Detection Protocols Toward PbS Nanoparticle-Labeled Signal Tagging

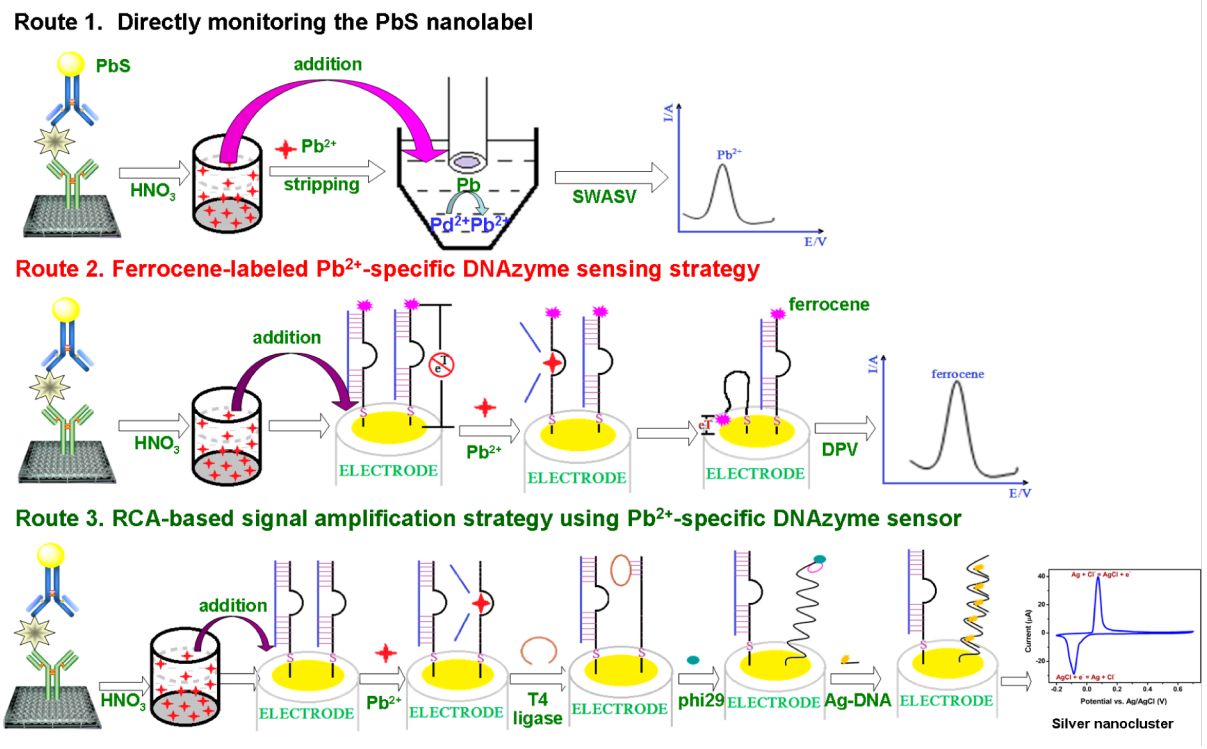

Scheme 1 presents the measurement process of a dual-nanostructure-based signal amplification strategy for the detection of AFP by using the rolling cycling amplification (RCA)-based amplification strategy. A high-binding polypropylene 96 well microtiter plate (ref. 655061, Greiner, Frickenhausen, Germany) was coated overnight at 4 °C with 50 μL per well of mAb_1 at a concentration of 10 μg mL^{-1} in a 0.05 M sodium carbonate buffer (pH 9.6). The microplate was covered with an adhesive plastic plate sealing film to prevent evaporation. On the following day, the plate was washed three times with washing buffer and then incubated with 300 μL per well of blocking buffer for 60 min at 37 °C with shaking. The plate was then washed as before. Following that, 50 μL of AFP standards/samples with various concentrations and 50 μL of the above-prepared PbS-pAb_2 suspension were simultaneously added into the microplate and incubated for 60 min at 37 °C under shaking. After washing again, a 20 μL aliquot of 1.0 M HNO_3 was added into each well to release lead ions from the PbS-pAb_2 (~3 min). The resulting acid solution containing the dissolved Pb^{2+} ions was transferred onto the DNAzyme-modified sensor and incubated for 70 min at RT. During this process, the liberated lead ions induced the specific cleavage of Pb-Sub on the DNAzyme. Following that, 5 μL of circular template DNA (1.0 nM) was dropped on the electrode and incubated for 30 min at 37 °C. After washing, the RCA reaction was initiated by dipping the electrode into 100 μL of phi29 DNA polymerase (2 unit mL^{-1}) reaction buffer (50 mM, pH 7.5 Tris-HCl buffer, 10 mM magnesium acetate, 33 mM potassium acetate, 1.0 mM dithiothreitol, 10 mM dNTP, and 0.1% Tween 20) and incubated for 60 min at 37 °C. Subsequently, the electrode was immersed into the above-prepared Ag-DNA and hybridized for 35 min at 37 °C. Finally, the differential pulse voltammetric (DPV) measurement was implemented in 10 mM Tris-HAc buffer +0.1 M KCl (pH 7.4) at an applied potential range of 0−0.4 V with a pulse amplitude of 20 mV and a pulse width of 50 ms on an AutoLab μAUTIII.FRA2.v electrochemical workstation (Eco Chemie, The Netherlands) with a conventional three-electrode system comprising a Pt-wire counter electrode, an Ag/AgCl reference electrode, and a modified gold working electrode. All incubations and measurements were conducted at room temperature (25 ± 1.0 °C). Analyses are always made in triplicate.

3. RESULTS AND DISCUSSION

For the conventional electrochemical immunoassays, metal sulfide nanoparticles are usually used for the labeling of the detection antibody because metal components yield well-resolved highly sensitive stripping voltammetric signals for the corresponding targets. The assay usually involves (i) preconcentration of a metal onto a solid electrode surface or into Hg (liquid) at negative potentials and (ii) selective oxidation of each metal species during an anodic potential sweep. Hence, use of mercury is usually necessary. In contrast, the emergence of a Pb^{2+}-specific DNAzyme sensor provides exciting new possibilities for advanced development of new analytical tools and instrumentation. Typically, metal sulfide nanoparticles consist of numerous metal ions, which can be used for the cleavage of metal ion-specific DNAzyme after dissolving by acid. The cleaved DNA fragment can be utilized as the template for molecular biological amplification, e.g., rolling cycling amplification and hybridization chain reaction.

In this work, the electrochemical signal mainly derived from the encapsulated AgNC in the Ag-DNA. To verify this issue, the as-prepared DNAzyme sensor was utilized for direct detection of lead ions. Experimental results indicated no peak currents were observed at the DNAzyme sensor, Pb^{2+}-cleaved DNAzyme sensor, and the RCA-amplified sensor (curve '*a*' in Figure 1A). Significantly, after the RCA-amplified sensor was

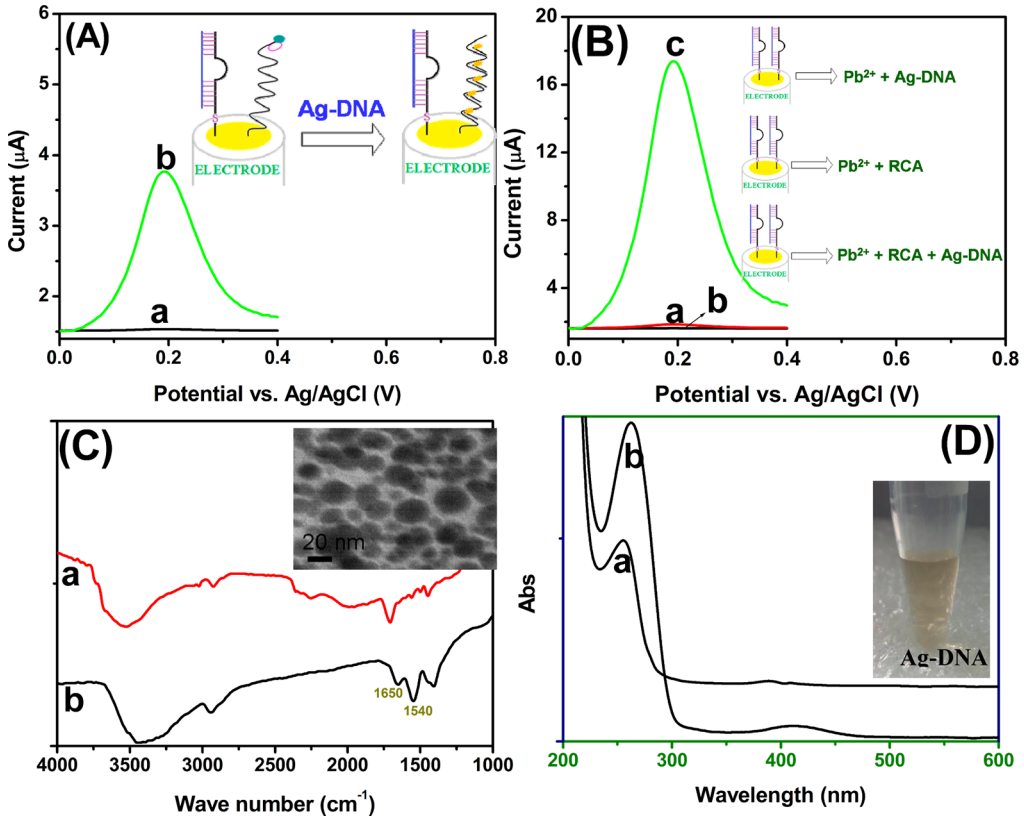

Figure 1. (A) DPV response curves of RCA-amplified DNAzyme sensor (a) before and (b) after hybridization with Ag-DNA in 10 mM Tris-HAc buffer + 0.1 M KCl (pH 7.4). (B) DPV response curves of the as-prepared DNAzyme sensor toward various substrates: (a) Pb^{2+} + Ag-DNA, (b) Pb^{2+} + (circular template DNA + phi29 DNA polymerase + dNTP), and (c) Pb^{2+} + (circular template DNA + phi29 DNA polymerase + dNTP) + Ag-DNA in 10 mM Tris-HAc buffer +0.1 M KCl (pH 7.4). (C) FTIR spectra of (a) PbS nanoparticles and (b) PbS-pAb_2 (inset: TEM image of PbS nanoparticles). (D) UV−vis absorption spectra of Ag-DNA (inset: prepared Ag-DNA).

incubated with Ag-DNA, a strong DPV peak current was appeared (curve '*b*' in Figure 1A). Logically, two puzzling questions to be produced were (i) whether the electrochemical signal originated from the specific reaction of the DNAzyme sensor and (ii) whether the rolling cycling amplification could be formed. As the control test, the as-prepared DNAzyme sensor was incubated with various components: (i) Pb^{2+} + Ag-DNA, (ii) Pb^{2+} + (circular template DNA + phi29 DNA polymerase + dNTP), and (iii) Pb^{2+} + (circular template DNA + phi29 DNA polymerase + dNTP) + Ag-DNA. As shown in from Figure 1B, Ag-DNA was not nonspecifically adsorbed onto the DNAzyme sensor after the immobilized DNAzyme was cleaved. Only if the RCA reaction was executed on the cleaved DNAzyme sensor, the Ag-DNA could not be hybridized onto the electrode. These results indicated that the dual-nanostructure-based amplification strategy could be preliminarily applied for the detection of AFP by coupling with the rolling cycling amplification.

The polyol process was involved in the preparation of PbS nanoparticles. The polyol, such as diethylene glycol (DEG), is a good solvent and can easily dissolve a variety of polar inorganic materials owing to its high permittivity (ε = 32) and boiling points. Meanwhile, it exhibits the reducing properties at high temperature.[31] PAA was chosen as the surfactant to produce highly water-soluble PbS nanoparticles. The carboxylate groups of PAA can show strong coordination power with the metal ions, and the carboxylate groups extending into aqueous solution can cross-link with an antibody. Upon introduction of thiourea (TU) into the mixture at ∼215 °C, a very fast decomposition of TU leads to the formation of plenty of S^{2-} in the system. Both nucleation and growth are involved in this procedure, and finally, metal sulfides were formed. Inset of Figure 1C shows a typical transmission electron microscope (TEM) of the carboxylated PbS nanoparticles. The mean size was 20 nm with a homogeneous dispersion in the distilled water.

Using the carbodiimide coupling method, the pAb_2 antibody could be covalently conjugated onto the surface of PbS nanoparticles. To demonstrate this point, PbS nanoparticles before and after modification with pAb_2 were studied by using Fourier transform infrared (FTIR, Nicolet 6700, U.S.A.) spectrometry (Figure 1C). As is well known, the shapes of the infrared absorption bands of amide I groups at 1610−1690 cm^{-1} corresponding to the C═O stretching vibration of peptide linkages and amide II groups around 1500−1600 cm^{-1} from a combination of N−H bending and C−N stretching can provide detailed information on the secondary structure of proteins.[32] As shown from curve '*b*', two absorption bands for amide I and amide II at PbS-pAb_2 were obtained at 1650 and 1540 cm^{-1}, respectively. Compared with curve '*a*', two characteristic peaks mainly derived from the labeled pAb_2.[32] The results revealed that a pAb_2 antibody could be bound to PbS nanoparticles by using the carbodiimide coupling method.

As mentioned above, the electrochemical signal mainly originated from the encapsulated silver nanocluster into the detection DNA probe. To monitor the successful preparation of the nanoclusters, a UV−vis absorption spectroscope was used. As shown from curve '*a*' in Figure 1D, one absorption

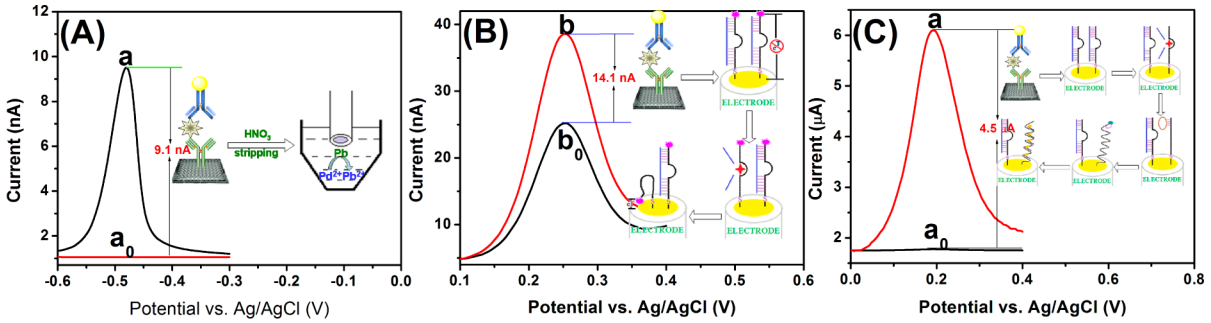

Figure 2. Comparison of DPV responses of variously assayed protocols toward (a_0) zero analyte and (a) 0.1 ng mL^{-1} AFP, by (A) directing monitoring the PbS nanolabels, (B) ferrocene-labeled Pb^{2+}-specific DNAzyme sensing strategy, and (C) RCA-based signal amplification strategy by coupling with Pb^{2+}-specific DNAzyme sensor.

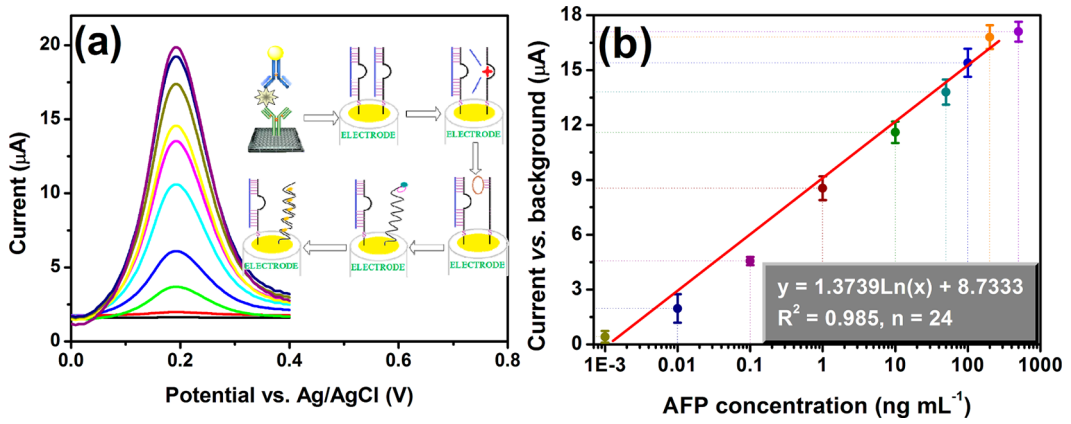

Figure 3. (a) Typical DPV response curves of the RCA-based signal amplification strategy in 10 mM Tris-HAc buffer +0.1 M KCl (pH 7.4) toward various concentration AFP standards: 0, 0.001, 0.01, 0.1, 1.0, 10, 50, 100, 200, and 500 ng mL^{-1} from bottom to top. (b) Relationship between DPV peak currents (vs background current) and AFP concentrations.

peak at 260 nm was observed at the detection DNA probe. After the detection probe was incubated with $AgNO_3$ and $NaBH_4$, two absorption peaks at 264 and 408 nm were obtained (curve '*b*'), which were from the DNA probe and reduced silver nanoclusters.[33,34] Meanwhile, the obvious difference between pure DNA and Ag-DNA could be clearly observed from the inserted photo in Figure 1D.

To elucidate the advantage of the dual-nanostructure-based signal amplification strategy over the existing methods, another two assay protocols were also used for the detection of AFP (0.1 ng mL^{-1} as an example): (i) directly monitoring the labeled PbS nanoparticles by using the square wave anodic stripping voltammetric (SWASV) method on a mercury drop electrode and (ii) monitoring the Pb^{2+}-induced DNAzyme cleavage by using ferrocene-labeled DNAzyme as molecular tag. The construction process and measurement methods were described in detail in our recent paper.[21] The judgment was based on the change in the peak current relative to zero analyte. As shown in from Figure 2, the immunoassay of using the labeled PbS nanoparticles as molecular tags exhibited a low change in the current relative to zero analyte (9.1 nA, curve '*a*' vs curve 'a_0' in Figure 2A), while that of using Pb^{2+}-specific DNAzyme sensor was 14.1 nA (curve '*b*' vs curve 'b_0' in Figure 2B). The reason might be that (i) the labeled ferrocene, as a good electron mediator, was greatly conducive to electron transfer between the supporting electrolyte and the base electrode and (ii) all the released lead ions from PbS nanolabels were not accumulated on the mercury drop electrode during a deposition step. More inspiringly, the electrochemical signal by using the dual-nanostructure-based signal amplification strategy could be further amplified (4500 nA, curve '*c*' vs curve 'c_0' in Figure 2C). This is most likely a consequence of the fact that one PbS nanoparticle accommodated many lead ions, and each lead ion could induce the cleavage of one DNAzyme, which could trigger the RCA reaction. The formed long DNA strand could hybridize more Ag-DNA molecular tags. In this case, a silver nanocluster on the probe was brought into close proximity to one AgNC on the neighboring probe. By this token, numerous silver nanoclusters were formed, each of which produced an electrochemical signal within the applied potentials, thereby resulting in the amplification of electrochemical signal.

Prior to quantitative determination, some experimental conditions influencing the analytical properties of the electrochemical immunoassay should be optimized. Experimental results indicated that the optimal parameters were 70 min for the cleavage of Pb^{2+}-specific DNAzyme, 60 min for the RCA reaction, and 35 min for hybridization of Ag-DNA, respectively. Under optimal conditions, the sensitivity and quantitative range of the electrochemical immunoassay were monitored toward AFP standards with various concentrations by using the designed routine. As shown from Figure 3a, the DPV peak currents increased with increasing AFP concentration in the sample. A linear dependence between the peak currents and the logarithm of AFP concentrations in the sample were acquired in the range from 1.0 pg mL^{-1} to 200 ng mL^{-1}, that is, over five decades. The detection limit (LOD) was 0.8 pg mL^{-1} at the $3S_{blank}$ level (where S_{blank} is the standard deviation of a blank

solution, n = 13), while the limit of quantification (LOQ) was 2.7 pg mL^{-1}.[35] Because the cutoff value of AFP in the human normal is about 10 ng mL^{-1}, the electrochemical immunoassay can completely meet the requirement of clinical diagnostics. Although the system has not yet been optimized for maximum efficiency, importantly, the LOD of the developed immunoassay was over 1000-fold lower than that of commercially available AFP ELISA kits (1.0 ng mL^{-1}, Genway Biotech., Inc.) (www.genwaybio.com).

To investigate the interfering effects of sample matrix components on the electrochemical responses of the developed immunoassays, we challenged the system with several possible components, such as carcinoembryonic antigen (CEA), prostate-specific antigen (PSA), thyroid-stimulating hormone (TSH), luteinizing hormone (LH), and human IgG. These samples were assayed by spiking them into blank human serum. The comparative study was carried out by measuring the low concentration of AFP analyte and high concentration of interfering components. As indicated from Figure 4, higher current was observed with the target AFP than that of other components. These results clearly demonstrated the high specificity of the developed immunoassay.

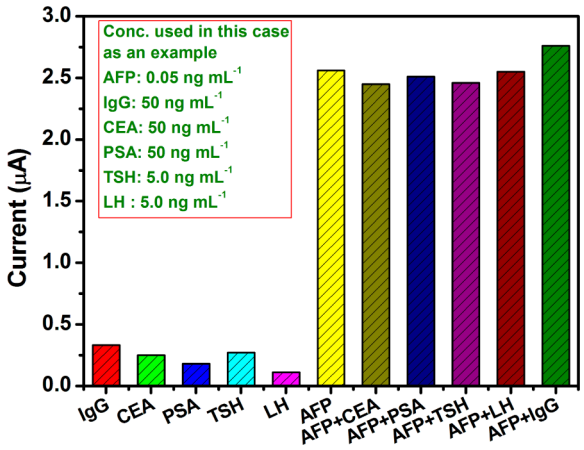

Figure 4. Specificity of the RCA-based signal amplification strategy. Initially, the human serum samples used for spiking were assayed by using the developed immunoassay, and various sample matrices were then spiked into the serum samples. Following that, the resulting mixtures were determined by using the same method under the same conditions.

Next, the precision of the developed immunoassay was monitored by assaying 0.1 and 10 ng mL^{-1} AFP as examples, using identical batches of DNAzyme sensors, PbS-pAb$_2$, and Ag-DNA. Experimental results indicated that the coefficients of variation (CVs, n = 3) of the intra-assay were 7.6 and 6.5% for 0.1 and 10 ng mL^{-1} AFP, respectively, whereas the CVs of the interassay with various batches were 9.8 and 9.2% toward the mentioned-above concentrations, respectively. Hence, both intra-assay and interassay verified acceptable reproducibility.

The accuracy of the electrochemical immunoassay was evaluated for testing 12 clinical serum specimens, which were collected from Fujian Provincial Hospital of China according to the rules of the local ethical committee. Prior to measurement, these samples were gently shaken at room temperature (Note: all handling and processing were performed carefully, and all tools in contact with patient specimens and immunoreagents were disinfected after use) and then evaluated by using the electrochemical immunoassay. The results were compared with those of the commercialized enzyme-linked immunosorbent assay (ELISA) method. The data between two methods were performed using a t-test for comparison of means preceded by the application of an F-test. As shown in Table 1, no significant

Table 1. Comparison of Assayed Results for Human Serum Specimens by Using Electrochemical Immunoassay and Referenced ELISA Method[a]

	method, conc. (ng mL^{-1}, mean ± SD, n = 3)[b]		
sample no.	found by electrochemical immunoassay	found by ELISA	t_{exp}
1	2.6 ± 0.4	3.3 ±0.3	2.42
2	13.5 ± 0.9	11.4 ± 1.3	2.30
3	2.7 ± 0.3	2.3 ± 0.2	1.92
4	5.7 ± 0.5	6.5 ± 0.6	1.77
5	0.6 ± 0.2	0.7 ± 0.2	0.61
6	18.5 ± 2.1	15.5 ± 1.3	2.10
7	6.1 ± 0.5	5.2 ± 0.4	2.43
8	1.1 ± 0.2	1.4 ± 0.2	1.83
9	20.9 ± 2	18.7 ± 1.6	1.48
10	35.7 ± 2.8	33.1 ± 1.6	1.39
11	27.3 ± 3.2	26.4 ± 2.7	0.37
12	53.4 ± 4.3	48.7 ± 2.9	1.57

[a]Regression equation (linear) for these data is as follows: y = 0.154 x + 0.911 (R^2 = 0.9984) (x-axis: by electrochemical immunoassay. y-axis: by the ELISA.) [b]Analyses were made in triplicate, and data were obtained based on the mean value of three assays (n = 3).

differences were encountered between the two methods at the 0.05 significance level because all the t_{exp} values in the case were less than t_{crit} ($t_{crit[4, 0.05]}$ = 2.77). Hence, the designed electrochemical immunoassay could be regarded as an optional scheme for detecting AFP in real samples.

4. CONCLUSION

This manuscript demonstrates an advanced electrochemical immunoassay protocol for sensitive detection of low-abundance protein (AFP used in this case) in biological fluids by coupling nano-amplification with a molecular biological amplification strategy. The highlight of this work is to realize the amplification of detectable signals toward low-abundance protein by coupling highly sensitive DNA sensors and highly selective immunosensors. Compared with conventional electrochemical immunoassays, the assay sensitivity (i.e., slope of the regression equation) is higher, although the assay routine is relatively complex. The merit of the high sensitivity can exactly identify two very close concentrations of target analyte, especially around the cutoff value. Future works should focus on designing and simplifying the assay protocol, e.g., by coupling with the sequential injection fluidic system.

AUTHOR INFORMATION

Corresponding Author

*Phone: +86-591-22866125; fax: +86-591-22866135; e-mail: dianping.tang@fzu.edu.cn).

Notes

The authors declare no competing financial interest.

ACKNOWLEDGMENTS

Support by the "973" National Basic Research Program of China (2010CB732403), Research Fund for the National

Science Foundation of Fujian Province (2011J06003), Doctoral Program of Higher Education of China (20103514120003), National Natural Science Foundation of China (21075019 and 41176079), and Program for Changjiang Scholars and Innovative Research Team in University (IRT1116) is gratefully acknowledged.

REFERENCES

(1) Ivanov, I.; Stojcic, J.; Stanimirovic, A.; Sargent, E.; Nam, R.; Kelley, S. *Anal. Chem.* **2012**, *85*, 398−403.
(2) Zhou, J.; Lai, W.; Zhuang, J.; Tang, J.; Tang, D. *ACS Appl. Mater. Interfaces* **2013**, DOI: 10.1021/am400652g.
(3) Martić, S.; Gabriel, M.; Turowec, J.; Litchfield, D.; Kraatz, H. *J. Am. Chem. Soc.* **2012**, *134*, 17036−17045.
(4) Li, Q.; Zeng, L.; Wang, J.; Tang, D.; Liu, B.; Chen, G.; Wei, M. *ACS Appl. Mater. Interfaces* **2011**, *3*, 1366−1373.
(5) Liu, B.; Zhang, B.; Cui, Y.; Chen, H.; Gao, Z.; Tang, D. *ACS Appl. Mater. Interfaces* **2011**, *3*, 4668−4676.
(6) Zhang, B.; Liu, B.; Tang, D.; Niessner, R.; Chen, G.; Knopp, D. *Anal. Chem.* **2012**, *84*, 5392−5399.
(7) Lu, L.; Zhang, X.; Kong, R.; Yang, B.; Tan, W. *J. Am. Chem. Soc.* **2011**, *133*, 11686−11691.
(8) Xia, F.; White, R.; Zuo, X.; Patterson, A.; Xiao, Y.; Kang, D.; Gong, X.; Plaxco, K.; Heeger, A. *J. Am. Chem. Soc.* **2010**, *132*, 14346−14348.
(9) Xia, Y.; Gan, S.; Xu, Q.; Qiu, X.; Gao, P.; Huang, S. *Biosens. Bioelectron.* **2013**, *39*, 250−254.
(10) Zhang, B.; Tang, D.; Goryacheva, I.; Niessner, R.; Knopp, D. *Chem.—Eur. J.* **2013**, *19*, 2496−2503.
(11) Pei, X.; Zhang, B.; Tang, J.; Liu, B.; Lai, W.; Tang, D. *Anal. Chim. Acta* **2013**, *758*, 1−18.
(12) Tang, D.; Cui, Y.; Chen, G. *Analyst* **2013**, *138*, 981−990.
(13) Dong, J.; Cui, X.; Deng, Y.; Tang, Z. *Biosens. Bioelectron.* **2012**, *38*, 258−263.
(14) Ding, C.; Wang, N.; Zhang, J.; Wang, Z. *Biosens. Bioelectron.* **2013**, *42*, 486−491.
(15) Liu, J.; Lu, Y. *J. Am. Chem. Soc.* **2007**, *129*, 9838−9839.
(16) Lu, C.; Wang, F.; Willner, I. *J. Am. Chem. Soc.* **2012**, *134*, 10651−10658.
(17) Wang, H.; Ou, L.; Suo, Y.; Yu, H. *Anal. Chem.* **2011**, *83*, 1557−1563.
(18) Shen, L.; Chen, Z.; Li, Y.; He, S.; Xie, S.; Xu, X.; Liang, Z.; Meng, X.; Li, Q.; Zhu, Z.; Li, M.; Chris Le, X.; Shao, Y. *Anal. Chem.* **2008**, *80*, 6323−6328.
(19) Xiao, Y.; Rowe, A.; Plaxco, K. *J. Am. Chem. Soc.* **2007**, *129*, 262−263.
(20) Yang, X.; Xu, J.; Tang, X.; Liu, H.; Tian, D. *Chem. Commun.* **2010**, *46*, 3107−3109.
(21) Zhang, B.; Liu, B.; Zhuang, J.; Tang, D. *Bioconjugate Chem.* **2013**, DOI: 10.1021/bc3006557.
(22) Hu, J.; Zhang, C. *Anal. Chem.* **2010**, *82*, 8991−8997.
(23) Cho, E.; Yang, L.; Levy, M.; Ellington, A. *J. Am. Chem. Soc.* **2005**, *127*, 2022−2023.
(24) Dong, H.; Wang, C.; Xiong, Y.; Lu, H.; Ju, H.; Zhang, X. *Biosens. Bioelectron.* **2013**, *41*, 348−353.
(25) Xue, Q.; Wang, Z.; Wang, L.; Jiang, W. *Bioconjugate Chem.* **2012**, *23*, 734−739.
(26) Hus, S.; Huang, Y. *Biosens. Bioelectron.* **2004**, *20*, 123−126.
(27) Tong, P.; Zhao, W.; Zhang, L.; Xu, J.; Chen, H. *Biosens. Bioelectron.* **2012**, *33*, 146−151.
(28) Zhao, Y.; Qi, L.; Chen, F.; Dong, Y.; Kong, Y.; Wu, Y.; Fan, C. *Chem. Commun.* **2012**, *48*, 3354−3356.
(29) Ji, H.; Yan, F.; Lei, J.; Ju, H. *Anal. Chem* . **2012**, *84*, 7166−7171.
(30) Dong, H.; Jin, S.; Ju, H.; Hao, K.; Xu, L.; Lu, H.; Zhang, X. *Anal. Chem.* **2012**, *84*, 8670−8674.
(31) Zhao, Y.; Li, C.; Li, F.; Shi, Z.; Feng, S. *Dalton Trans.* **2011**, *40*, 583−588.
(32) Li, Q.; Tang, D.; Tang, J.; Su, B.; Huang, J.; Chen, G. *Talanta* **2011**, *84*, 538−546.
(33) Kong, H.; Jang, J. *Langmuir* **2008**, *24*, 2051−2056.
(34) Zinchenko, A.; Baigl, D.; Chen, N.; Pyshkina, O.; Endo, K.; Sergeyev, V.; Yoshikawa, K. *Biomacromolecules* **2008**, *9*, 1981−1987.
(35) Zhang, B.; Hou, L.; Tang, D.; Liu, B.; Li, J.; Chen, G. *J. Agric. Food Chem.* **2012**, *60*, 8974−8982.